A Model for Process-Based Crash Simulation

Lademo, O.-G.[1, 4], Berstad, T.[1, 4], Tryland, T. [2], Furu, T.[3], Hopperstad, O.S.[4], Langseth, M.[4]

[1] *SINTEF Materials and Chemistry, N-7465 Trondheim, Norway.*
[2] *Hydro Aluminium Structures, N-2831 Raufoss, Norway.*
[3] *Hydro Aluminium R&D, N-6600 Sunndalsøra, Norway*
[4] *Structural Impact Laboratory (SIMLab)*
Department of Structural Engineering, Norwegian University of Science and Technology
N-7491 Trondheim, Norway.

Abstract

Manufacturing of a bumper system from aluminium extrusions often involves series of forming operations performed in the soft W temper condition, and then artificially age-hardening the components to the material's peak hardness T6 condition. It is perceptible that correct numerical representation of the crash performance of the resulting systems must rely upon a geometry obtained from a model following the process route, i.e. including simulation of all major forming operations. However, the forming operations also result in an inhomogeneous evolution of some internal variables (among others the effective plastic strain) within the shaped components. Here, results from tensile tests reveal that plastic straining in W-temper results in a significant change of the hardening curves (alloy and ageing-dependent increase or decrease in strength) as a function of plastic pre-straining. In addition, the tests revealed that the plastic deformation led to a reduction of the elongation of the T6 specimens. These data were obtained by uniaxial stretching of plates in the W temper to different levels of plastic deformation, sub-sequent artificial ageing to obtain T6 characteristics, machining of uniaxial tensile test coupons and, finally, testing until failure.

In the present work, these process effects have been included in a user-defined elasto-viscoplastic constitutive model incorporating a state-of-the-art anisotropic yield criterion, associated flow rule, non-linear isotropic and kinematic hardening rules, a strain-rate hardening rule as well as some ductile fracture criteria. To demonstrate and asses the modelling methodology, a 'through-process analysis' of the uniaxial tensile tests is performed. The pre-stretching of the plates in W temper is modelled with shell elements having an initial random Gauss-distributed thickness and stretched to different levels of plastic strain – comparable to the experimental ones - using the explicit solver of LS-DYNA. Then, uniaxial tensile specimens are trimmed from the deformed plates using the trimming option available in LS-DYNA. Next, strain dependent T6 properties are specified, after which the resulting specimens are stretched until instability and failure. Finally, the model assumptions are assessed by comparing engineering stress-strain curves obtained from the simulations and experiments.

Introduction

Robust design and production of light but crashworthy structural components in aluminium for the automotive industry are challenging tasks, involving development of alloys and manufacturing processes, structural design and crashworthiness analysis. In order to reduce the time needed to develop a competitive new product, it is necessary to apply non-linear finite element analysis to design the manufacturing process and to evaluate the crashworthiness of the final component. Prior studies have shown that aluminium alloys used in automotive applications have complex mechanical properties with anisotropic strength and ductility and that it may be necessary to use relatively complicated constitutive models to obtain the required accuracy in the numerical analyses [1][2][3][4][5][6][7][8].

The focus of the present paper is, however, that the manufacturing of a bumper system from aluminium extrusions often involves series of forming operations performed in the soft W temper condition, and then artificially age-hardening the components to the material's peak hardness T6 condition. It is perceptible that correct numerical representation of the crash performance of the resulting systems must rely upon a geometry obtained from a model following the process route, i.e. including simulation of all major forming operations. However, the forming operations also result in an inhomogeneous evolution of some internal variables (among others the effective plastic strain) within the shaped components. As will be seen, results from tensile tests reveal that plastic straining in W-temper results in a significant change of the hardening curves as a function of plastic pre-straining.

Experiments

An experimental study of uniaxial tensile tests aimed at investigating the effect of the shaping process on the material's peak hardness (temper T6) characteristics has been performed. These data were obtained by uniaxial stretching of plates in the W temper to different levels of plastic deformation, sub-sequent artificial ageing to obtain peak hardness characteristics, machining of uniaxial tensile test coupons and, finally, testing these specimens until instability and failure.

Figure 1 shows the resulting T6 properties for two of the investigated alloys. Clearly, the experiments reveal that plastic straining in W-temper results in a significant change of the peak hardness hardening curves. For the peak-aged 7003 alloy shown in part a) of the figure the pre-deformation reduces the yield stress by approximately 15%, while a strength increase of 10% is obtained for the under-aged 6060 alloy presented in part b) of the same figure. In addition, it is seen that the elongation of the T6 specimens is significantly reduced for both alloys.

For the first percentages of plastic strain the hardening curves could be judged 'reasonably parallel', but for higher plastic strains the tangent modulus for the pre-deformed material is less than for the un-deformed material. Previous studies have revealed that damage is negligible for the deformation levels at hand [5], so that the reduced hardening and ductility must be described by other means. The formability modelling technique presented by Berstad et al. [7] relies upon the instability theory of Marciniack and Kuczynski [9] that describes plastic instability as a result of inhomogeneity growth. One explanation – or at least contributing factor – to the reduced ductility could be that the plastic pre-deformation leads to a significant inhomogeneity growth that, when aged to temper T6 conditions, gives a strong localisation tendency. Alternatively, the hardening modulus could, as the yield stress, be directly affected by the plastic pre-deformation. To judge between these effects, a 'through-process' analysis of the experimental series is performed.

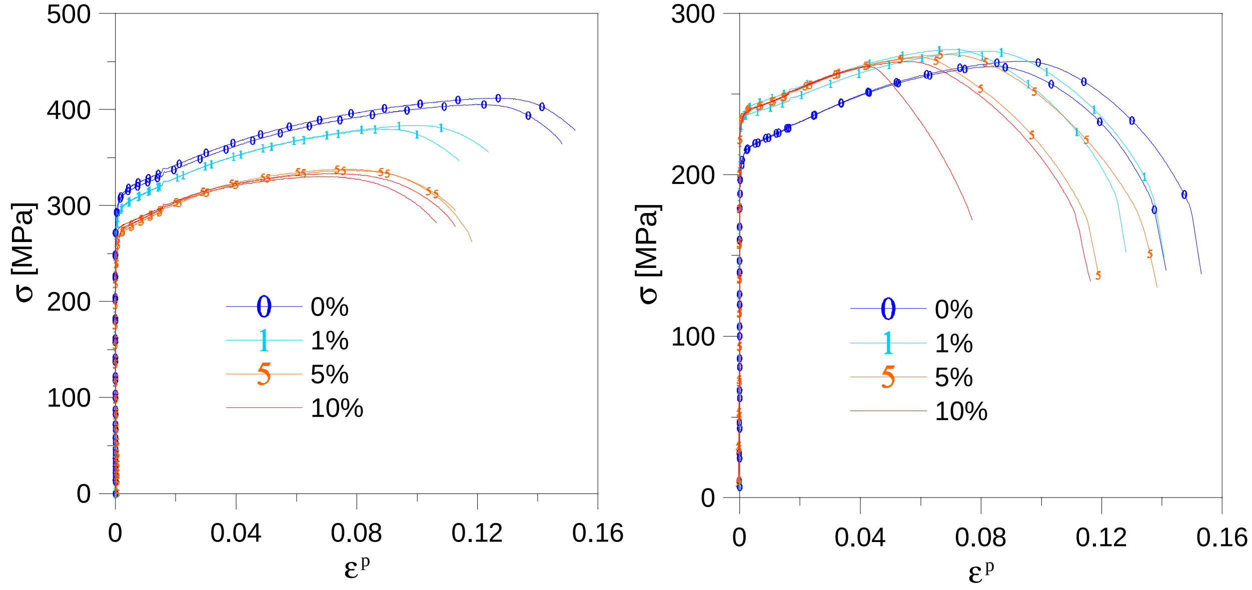

a) b)

Figure 1 Examples on the effect of plastic deformation in forming state (W) on end properties (T6). True stress vs. true plastic strain for a) peak aged 7003 alloy and b) under-aged 6060 alloy (1 hour storing at room temeprature between pre-deformation and artificial ageing, 2 parallel tests presented for each deformation level).

Constitutive Modeling

In the present work, the above-mentioned process effects have been included in a previously developed user-defined elasto-viscoplastic constitutive model incorporating a state-of-the-art anisotropic yield criterion, associated flow rule, non-linear isotropic and kinematic hardening rules, a strain-rate hardening rule as well as some ductile fracture criteria. The model is presented in detail by Berstad et al. [7] elsewhere in these proceedings.

The yield function f, which defines the elastic domain in stress space, is expressed in the form

$$f = \bar{f}(\boldsymbol{\sigma}) - \left(\sigma_Y + R\right) \le 0 \tag{1}$$

where σ_Y is the reference yield stress, R is the strain hardening variable, while the convex function $\bar{f}$ is defined by the chosen yield criterion. In the present work the Weak Texture Model (see Berstad et al. [7]) based on the yield criterion of Barlat and Lian [10] has been utilised. Further, only isotropic hardening has been considered where the strain hardening has been defined by

$$R = \sum_{i=1}^{2} Q_{Ri}(1 - \exp(-C_{Ri}\bar{\varepsilon})) \tag{2}$$

where $\bar{\varepsilon}$ is the accumulated plastic strain and Q_{Ri} and C_{Ri} are strain hardening constants. Strain-rate dependency has been neglected in the present study.

As discussed above, two different models have been developed to account for the demonstrated process effects. In modelling approach (i), only the yield stress σ_Y was assumed to be influenced by plastic straining in W temper, i.e. *the strain hardening* R *was assumed unaffected*. Figure 2 shows the reference yield stress in temper T6 as function of effective plastic straining in W temper (denoted $\bar{\varepsilon}^W$) relative to the yield stress of an un-deformed material (deduced from the results in Figure 1). Above 5% plastic strain the effect on the yield stress is assumed to be constant.

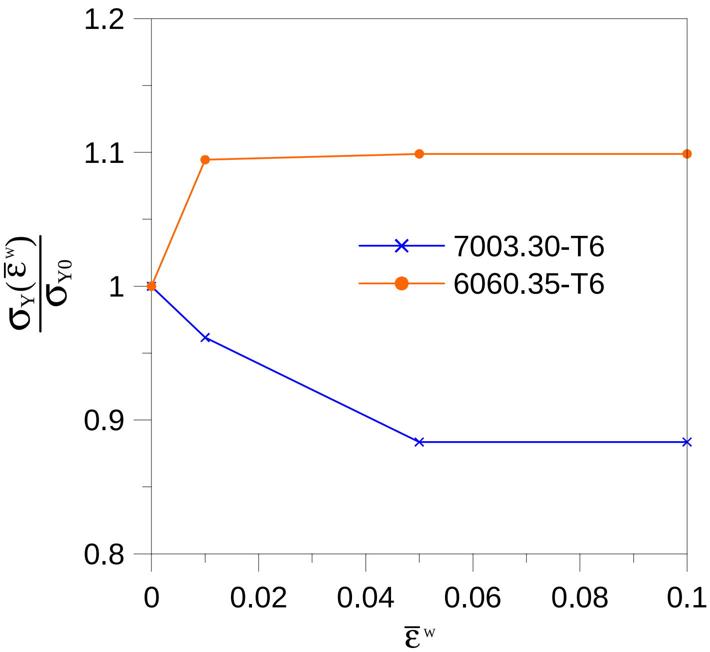

Figure 2 Reference yield stress as function of effective plastic straining in W temper relative to the yield stress of an un-deformed material.

In modeling approach (ii) all hardening curves shown in Figure 1 were fitted to the hardening rule given by Eqs. (1) and (2). For plastic strains in between the experimental data of 0%, 1%, 5% and 10%, reference hardening curves were found by linear interpolation between the prescribed curves.

Validation Analyses

To demonstrate and assess the modeling methodology, a 'through-process analysis' of the pre-deformed uniaxial tensile tests was performed. The pre-stretching of the plates in W temper was modelled with 13500 shell elements having an initial random Gauss-distributed thickness with a coefficient of variation of the thickness $\mathrm{CoV}(t) = 0.005$, and stretched to different levels of plastic strain – comparable to the experimental ones - using the explicit solver of LS-DYNA.

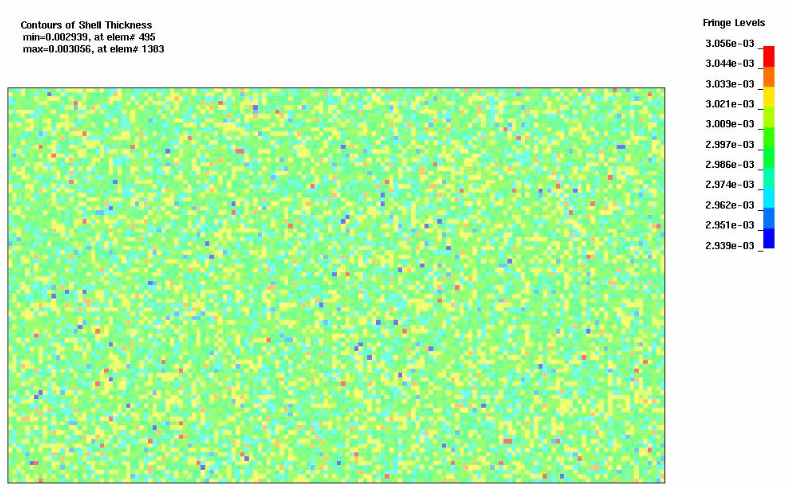

Figure 3 FE-model with initial thickness inhomogeneity for pre-stretching analysis (soft W temper).

Then, as illustrated in Figure 4, uniaxial tensile specimens were trimmed from the deformed plates using the trimming option available in LS-DYNA [11], transferring the resulting effective plastic strain and thickness distribution.

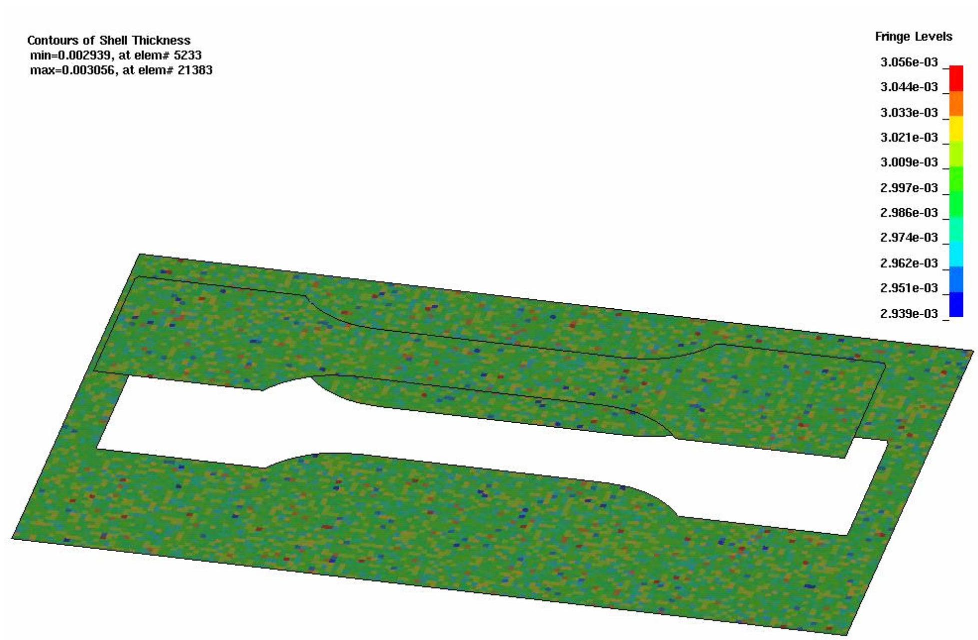

Figure 4 Trimming of specimens from plate stretched to different levels of plastic strains.

Next, strain dependent T6 properties were specified according to approach (i) and (ii), after which the resulting specimens were stretched until instability and failure. For the present study the local failure criterion is based upon a critical thickness strain determined from the experiments.

In order to asses the modeling approaches, experimental and numerical engineering stress-strain curves are compared. Figure 5 presents the results using modeling approach (i) where only the yield stress was assumed to be influenced by the pre-deformation. For the 7003 material, shown in part a) of the figure, the instability for the un-deformed reference condition occurs somewhat too early. For the 6060 material, shown in part b) of the same figure, a reasonably accurate prediction of the onset of plastic instability is obtained for the un-deformed reference condition. For the pre-deformed specimens the instability occurs only slightly later (7003) or earlier (6060) than for the un-deformed condition, but is mainly to be subscribed to the decreased and increased stress levels, respectively. For both materials, the effect of initial inhomogeneity and corresponding inhomogeneity growth predicted with the present constitutive equation and parameters is thus insufficient to explain the reduced elongation. For the 6060 material it is also seen that the hardening at different levels of plastic pre-deformation *is* significantly different than for the un-deformed material. Further, for both materials the 'tail' of the curve is somewhat too steep, indicating that the strain localisation is too rapid in the analyses. Two effects could contribute to and explain this latter effect

- the anisotropy representation obtained with the Weak Texture Model could be too inaccurate.
- a positive strain-rate sensitivity, which is not accounted for in the constitutive equation, would delay the instability significantly. This could also explain the discrepancy for the un-deformed 7108 test specimen.

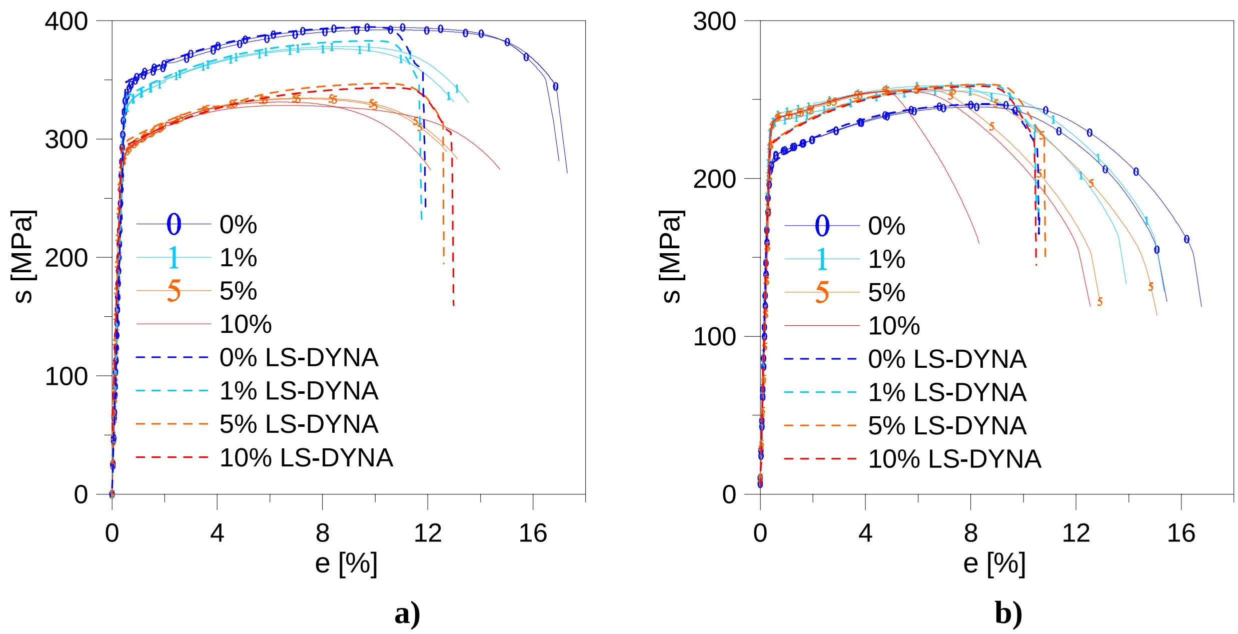

Figure 5 Experimental vs. numerical engineering stress-strain curves obtained with modeling approach (i), a) 7003 alloy and b) 6060 alloy.

Figure 6 presents corresponding results obtained using modeling approach (ii) where different yield stress and hardening parameters σ_Y, Q_{Ri} and C_{Ri} were prescribed for the four levels of pre-deformation. Clearly, this modeling approach catches the reduced elongation with respect to pre-deformation much better than modeling approach (i), but the tail of the curves is still too steep.

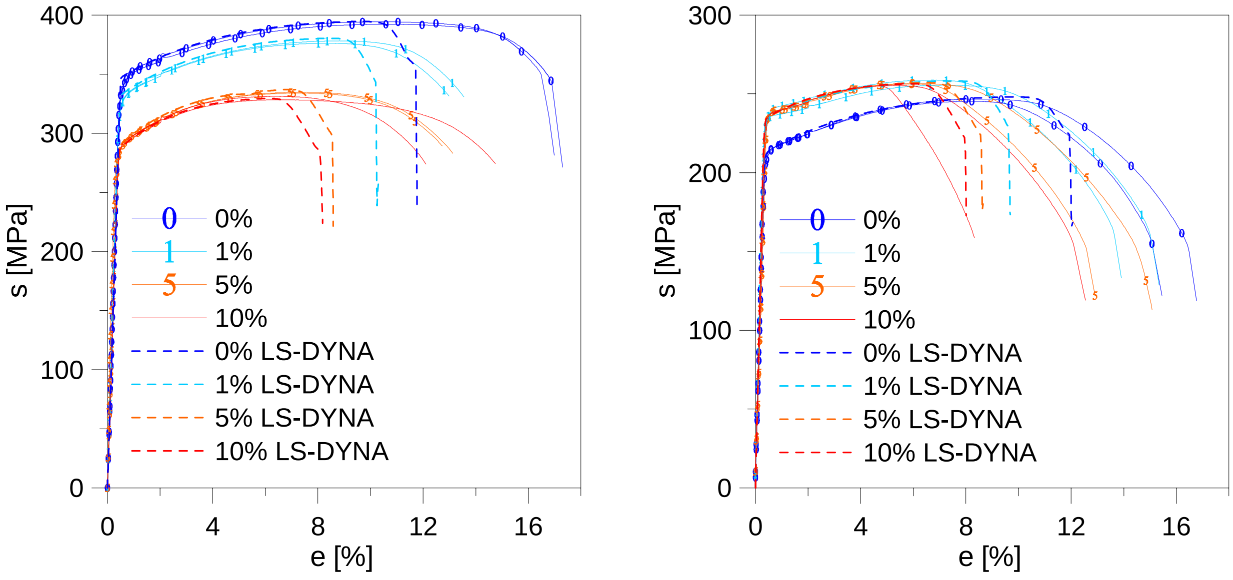

a) **b)**

Figure 6 Experimental vs. numerically obtained engineering stress-strain curves obtained with modeling approach (ii), a) 7003 alloy and b) 6060 alloy.

Conclusions

In the present work, two approaches for inclusion of process effects in an existing user-defined elasto-viscoplastic constitutive model have been investigated. To demonstrate and asses the modelling methodology, a 'through-process analysis' of the uniaxial tensile tests was performed. Based upon the analyses with modeling approach (i) it was concluded that the effect of initial inhomogeneity and corresponding inhomogeneity growth (as predicted with the present constitutive equation and parameters) was insufficient to explain the reduced elongation as function of pre-straining. The refined modeling approach (ii), – where also strain hardening of the material was assumed to be influenced by the pre-deformation – clearly captures the reduced elongation with respect to pre-deformation much better than modeling approach (i).

For all analyses the tail of the curves is too steep, indicating that the strain localisation is too rapid in the analyses. This could be due to inaccurate anisotropy representation offered by the Weak Texture Model and/or a positive strain-rate sensitivity, which presently is not accounted for in the constitutive equation.

Acknowledgement

The financial support from Hydro Aluminium Structures and the Norwegian Research Council is highly appreciated.

References

[1] F. Barlat, Y. Maeda, K. Chung, M. Yanagawa, J.C. Brem, Y. Hayashida, D.J. Lege, K. Matsui, S.J. Murtha, S. Hattori, R.C. Becker and S. Makosey, Yield function development for aluminum alloy sheets, J. Mech. Phys. Solids, 45 (1997) 1727-1763.

[2] O.-G. Lademo, O.S. Hopperstad, M. Langseth, An evaluation of yield criteria and flow rules for extruded aluminium alloys, Int. J. Plasticity 15 (1999) 191-208.

[3] O.-G. Lademo, O.S. Hopperstad, M. Langseth, “On the Strain-Rate Effect and Anisotropy of AA7108”, 3rd International Symposium on Impact Engineering, Singapore, 7-9 December.

[4] T. Berstad, O.S. Hopperstad, O.-G. Lademo, K.A. Malo, “Computational model of ductile damage and fracture in shell analysis“, Second European LS-DYNA Conference, Gothenburg, June 14-15, 1999.

[5] O.-G. Lademo, O.S. Hopperstad, T. Berstad, M. Langseth, Prediction of plastic instability in extruded aluminium alloys using shell analysis and a coupled model of elasto-plasticity and damage, Accepted for publication in Journal of Materials Processing Technology, February 2003.

[6] O.-G. Lademo, O.S. Hopperstad, K.A. Malo, K.O. Pedersen, ”Modelling of Plastic Anisotropy in Heat-Treated Aluminium Extrusions”, **125-126**, pp. 84-88, Journal of Materials Processing Technology.

[7] T. Berstad, O.-G. Lademo, O.S. Hopperstad, K.A. Malo, K.O. Pedersen, "Formability modelling with LS-DYNA", 8th International LS-DYNA User's Conference, Detroit, May 3-5, 2004.

[8] O.-G. Lademo, (1999). “Engineering Models of Elastoplasticity and Fracture for Aluminium Alloys“, Dr.ing. thesis 1999:39, Department of Structural Engineering, Norwegian University of Science and Technology, Trondheim, Norway.

[9] Z. Marciniak and K. Kuczynski, Limit strains in the processes of stretch-forming sheet metal, Int. J. Mech. Sci. 9 (1967) 609 - 620.

[10] F. Barlat and Lian, “Plastic Behaviour and Stretchability of Sheet Metals. Part I: A Yield Function for Orthotropic Sheets under Plane Stress Conditions”, International Journal of Plasticity, **5**, pp. 51-66.

[11] Livermore Software Technology Corporation (LSTC), LS-DYNA Keyword User’s Manual, Version 970, 2003.